SIMULATION OF MARTIAN DUST ACCUMULATION ON SURFACES

Marla E. Perez-Davis and James R. Gaier
National Aeronautics and Space Administration
Lewis Research Center
Cleveland, Ohio 44135

Robert Kress
University of Akron
Akron, Ohio 44311

Justus Grimalda
Massachusetts Institute of Technology
Boston, Massachusetts 02139

ABSTRACT

Future NASA space missions include the possibility of manned landings and exploration of Mars. Environmental and operational constraints unique to Mars must be considered when selecting and designing the power system to be used on the Mars surface.

This paper describes a technique which has been developed to simulate the deposition of dust on surfaces. Three kinds of dust materials were evaluated: aluminum oxide, basalt, and iron oxide. The apparatus was designed using the Stokes and Stokes-Cunningham law for particle fallout, with additional consideration given to particle size and shape.

Characterization of the resulting dust films on silicon dioxide, polytetrafluoroethylene, indium tin oxide, diamondlike carbon, and other surfaces are discussed based on optical transmittance measurements. The results of these experiments will guide future studies which will consider processes to remove the dust from surfaces under Martian environmental conditions.

INTRODUCTION

In the forseeable future, a manned mission will land on the surface of Mars. Environmental and operational constraints unique to Mars need to be considered when selecting and designing the power system to be used on the Martian surface.

The natural environmental characteristics of Mars, such as dust, ultraviolet radiation, winds, temperature variations, atmospheric condensates and/or synergistic combinations of these, may pose a threat to the power systems established on the Martian surface. Most of the current information on the characteristics of the Martian atmosphere and soil composition was obtained from the Viking 1 and 2 missions in 1976. The Viking landers found that the Martian atmosphere is composed of CO_2 (95.5 percent), N_2 (2.7 percent), Ar (1.6 percent), O_2 (0.15 percent), and CO (0.07 percent) (ref. 1).

The Martian atmosphere contains suspended dust particles which result from many local and global dust storms that occur each year. The information obtained from the Mariner 9 and the Vikings missions suggest that the dust is a mixture of many

materials such as granite, basalt, basaltic glass, obsidian, quartz, andesite, or montmorillonite. Viking Landers' results also suggest the presence of highly oxidizing species (ref. 2).

Space power system components such as photovoltaic arrays, radiators, and solar concentrators are vulnerable to degradation in the Martian environment. Accumulation of dust particles may reduce the transmittance of photovoltaic arrays or reduce the thermal emittance of radiators thus permanently degrading their performance. Abrasion of power surfaces could also result from dust blown by the wind.

This paper describes a technique which has been developed to simulate the deposition of dust on surfaces on Mars. Characterization of the resulting dust films on various surfaces will also be discussed. The results of these experiments will guide future studies which will consider processes to remove the dust from surfaces under Martian conditions.

The authors would like to thank Bruce Banks, Chief of the Electro-Physics Branch at NASA Lewis Research Center for his constructive criticism and suggestions in the design and fabrication of the dust box and Kim De Groh for helping with the SEM pictures. Appreciation is also expressed to Robert Martineau from the Materials Divison at NASA Lewis Research Center for providing the particle size analyses of all our dust material.

APPROACH

Materials

The observations made by the Viking lander imaging cameras on Mars were used to estimate dust particle size and composition. The fine-grained material in the atmosphere is considerably less than 100 μm in diameter. Three different dust composition materials were considered in this simulation. The first dust was 1800 grit optical grinding material from American Optical Company. The particle size ranged from 0.1 to 25 μm with a particle size distribution as shown in figure 1. The composition is principally aluminum oxide powder (89 percent), with significant amount of silicon dioxide (6.6 percent) and titanium dioxide (3 percent), and small amounts of iron (III) oxide (0.6 percent) and chromium (III) oxide (0.6 percent). The particles have a density of 3.67 g/cm^3. The sample materials dusted included candidate materials for photovoltaic arrays and radiators. The photovolataic arrays samples were 1 in. (2.54 cm) square, 5 mil (0.13 mm) thick coverslips left bare or coated with silicon dioxide (SiO_2), polytetrafluoroethane (PTFE), 50 percent SiO_2 - PTFE, indium tin oxide (ITO), or diamond-like carbon (DLC). The radiator samples used were 1 in. (2.54 cm) diameter discs of carbon-carbon composite, pyrolytic graphite, or arc-textured copper.

The second type of dust was a basalt (trap rock) with the following composition (percent by weight): SiO_2 (46.6), Al_2O_3 (16.6), Fe_2O_3 (13.0), CaO (11.1), MnO (0.3), MgO (6.1), No_2O (2.3), K_2O (1.1), TiO_2 (2.0), CO_2 (0.1), and P_2O_5 (0.1). Glass coverslips were dusted with the trap rock of 3.0 g/cm^3. The particle size distribution of this material is shown in figure 2.

Iron oxide (Fe_2O_3) particles (2.83 g/cm^3) were the third dust type deposited on glass coverslips. Figure 3 presents the particle size distribution of these particles.

METHOD

The forces of a particle falling through air are primarily those of weight in the direction of motion and the aerodynamic drag opposition. Figure 4 illustrates the forces acting on a spherical particle. The general solution of the equation in terms of the terminal velocity (V_t) is:

$$V_t = \frac{g d_p^2 (\rho_p - \rho_g)}{18\ \mu} \tag{1}$$

where g is gravity, d_p is particle diameter, μ is viscosity of fluid, and ρ_p, ρ_g are density of the particle and fluid, respectively.

This expression is known as Stokes' law. This equation is quite accurate for spherical particles of diameters <50 μm; for particles <5 μm in diameter, a multiplicative correction factor (ref. 3), K_c, is often applied given by:

$$K_c = 1 + \frac{2}{d_p}\left[1.257 + 0.40\ \exp\left(-\frac{0.55\ d_p}{\lambda}\right)\right] \tag{2}$$

here λ is the mean free path of the molecules in the gas phase defined by:

$$\lambda = \frac{\mu}{0.499\ u_m}$$

where u_m is the mean molecular speed, μ is the viscosity of the gas, and ρ is the gas density. Using the kinetic theory of gas u_m is defined by:

$$u_m = \left(\frac{8\ RT}{\pi M}\right)^{1/2} \tag{3}$$

where M is the molar mass or molecular weight of the gas. This correction factor is used because the mean free path of the gas molecules in the atmosphere approaches the particle diameter for particles smaller than 5 μm in diameter. These small particles tend to slip past the gas molecules causing the terminal velocity to become greater than that predicted by Stokes' law. The relation used for these small particles is known as the Stokes-Cunningham law:

$$V_c = K_c V_t \tag{4}$$

The above equations were used to determine an approximate and reasonable height for the design and fabrication of a box to be used for the deposition of dust on sample surfaces. Figure 5 shows the terminal velocity of particles in atmospheric air at room temperature. A height of 0.7 m was selected, and the falling time for different particle sizes was calculated. Figure 6 shows the falling time for different particle sizes at the height of 0.7 m.

The dust particles were elevated by an air pulse blowing downward on the dust material. In order to reduce the aggregation of particles due to moisture, a moisture trap was inserted in the air line. The dust box was constructed of stainless steel (fig. 7) and consists of a square pyramidal recirculating chamber, a dusting chamber, a tray for samples, transparent windows, and the air lines. The purpose of the conical shape is to ensure the collection and distribution of the dust in a more uniform and efficient manner. In designing the recirculating chamber, careful

attention was given to the selection of the required angle to overcome the friction so the particles would slide and be collected at the bottom of the box. Theoretical and experimental calculations showed that the required angle should be >40° and <90°, so based on these results the cone box angle selected was 64°. The transparent closed windows at opposite sides of the dust box were used to measure optical transmittance of the dust through the box.

Optical transmittance measurements were made using a transmittance measurement device (TMD). The TMD is made up of a white light source and a sensing head of a Coherent Model 212 Power Meter. Absolute transmittance measurements were converted into percent transmittance measurements. Measurements were made of the occlusion of light through the windows of the dust box at the beginning of each dusting simulation and of the samples before and after dusting.

The samples were mounted in specially designed sample holders (fig. 8), which tilt at different angles, 0°, 22.5°, 45°, 67.5°, or 90° from the floor. All the sample holders were held horizontally and subject to a dusting which simulates the aftermath of a dust storm.

The sample tray was inserted into the dusting chamber 30 sec after the dust was elevated to avoid collecting particles >20 μm (fig. 6).

RESULTS AND DISCUSSION

There are several factors which will effect the dusting process including particle size, particle shape, surface chemistry, amount of dust, and time. The particle sizes utilized in the dusting process were the ones which expected to become suspended during a global or local dust storm, but when normal weather conditions return, will settle out. It is important to note that Stokes-Cunningham fallout is probably not the dominant mechanism leading to dust storm clearing at Mars. Particles between 1 to 10 μm suspended in the Martian atmosphere are more likely supported by turbulence with an eddy diffusion coefficient and do not experience the Stokes-Cunningham fallout (ref. 4). It is thought that these particles are mixed into the surface boundary layer where they impact the surface and fallout.

Examination of our experimental particles using the scanning electron microscope (SEM), showed a nonspherical shape (fig. 9). Evidence suggests that dust particles on Mars are also nonspherical (ref. 5), which makes our powder dust appropiate for the expected size and shape of the Martian dust. The chemistry of our dust, however, is not expected to be similar to Martian dust (ref. 4). The settling time of about 8 min for Al_2O_3 was selected in order to collect different particle sizes and also to reduce the transmittance of the samples. The settling time of 8 min for trap rock or iron oxide was not enough to get the same occlusion of light obtained for aluminum oxide dusted samples. Two settling runs were needed to obtain similar occlusion for samples dusted with trap rock and several runs were needed for the ones dusted with the iron oxide.

The samples were weighed before and after dusting, however, the weight of the dust added to the surface was below the sensitivity of the balance used (±0.1 mg). Examination of the dusted samples using SEM analysis showed a very evenly distributed dust layer and some particle aggregation (fig. 10).

The uniformity of the dust deposited on the samples as function of the number of sequential dust elevation and depositions (dusting runs) are shown in figures 11 and 12. The transmittance of the samples after being dusted (T_d) divided by the initial transmittance (T_o) was used to characterize uniformity of the samples. The uniformity of dust deposition by materials (photovoltaic candidate materials), is shown in figure 12. A variety of transmittance values were obtained for each sample batch. Several factors, such as amount of dusting material in the dust box (initially 150 g were deposited in the box), type of dust, time of inserting the samples, and duration of dust deposition in the box (which is directly related to particle size collected) could account for the differences in transmittance.

CONCLUSIONS

The technique developed to dust samples was successfully tested. The process was applied to candidate materials to be tested at MARSWIT for aeolian study. It was found that dust is uniformly distributed over the samples, however the transmittance values of the samples shows different values for different runs. This difference is probably related to the fact that the amount of dust (grams) changes slightly after each run. Additional material was added after each run to compensate for the lost dust. Increases in transmittance loss might be related to the increase in dust material and reduction could indicate loss of material inside the box when compared occlusion by the same type of dust material. Also, exposure times are critically related to the particle sizes collected and consequently the light occlusion obtained as is the case for iron oxide particles.

REFERENCES

1. Owen, T.C., Biemann, K., Rushneck, D.R., Biller, J.E., Howarth, D.W., and Lefleur, A.L., "The Composition of the Atmosphere at the Surface of Mars," Journal of Geophysical Research, Vol. 82, No. 28, Sept. 30, 1977, pp. 4635-4639.

2. Huguenin, R.L., Miller, K.J., and Harwood, W.S., "Frost-Weathering on Mars: Experimental Evidence for Peroxide Formation," Journal of Molecular Evolution, Vol. 14, Dec. 1979, pp. 103-132.

3. Wark, K., and Warner, C.F., Air Pollution: Its Origin and Control, 2nd Edition, Harper & Row, New York, 1981.

4. Toon, O.B., Pollack, J.B., and Sagan C., "Physical Properties of the Particles Composing the Martian Dust Storm of 1971-1972," Icarus, Vol. 30, No. 4, Apr. 1977, pp. 663-696.

5. Zurek, R.W., "Martian Great Dust Storms: An Update," Icarus Vol. 50, No. 2-3, May-June 1982, pp. 288-310.

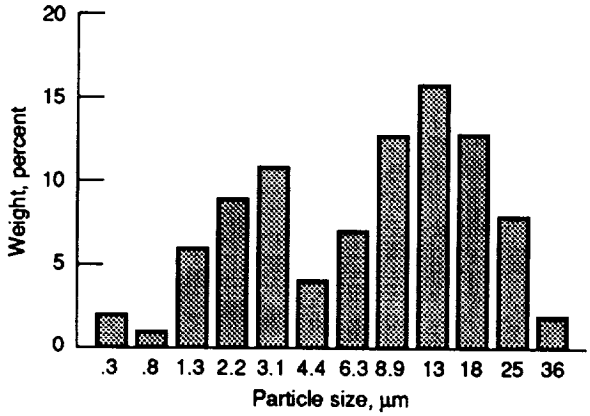

Figure 1.—Particle size distribution of aluminum oxide dust.

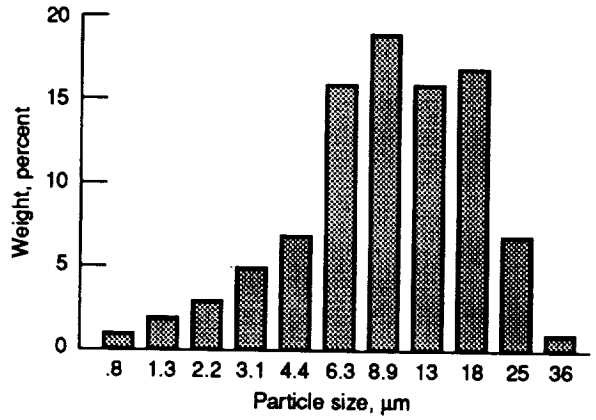

Figure 2.—Particle size distribution of basalt (trap rock).

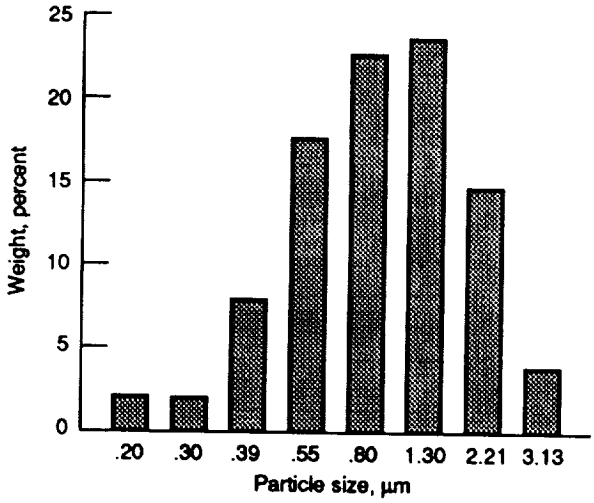

Figure 3.—Particle size distribution of iron oxide dust.

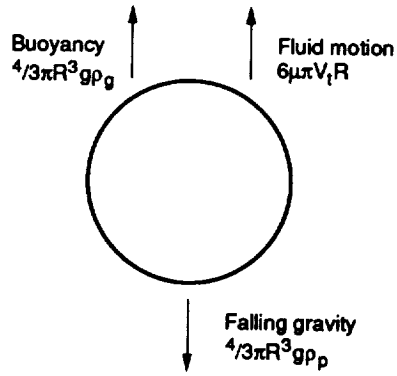

Figure 4.—Diagram of forces acting on a sphere.

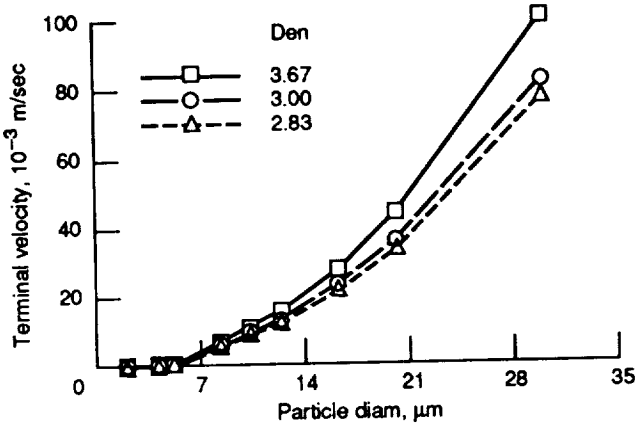

Figure 5.—Terminal velocity as a function of particle size.

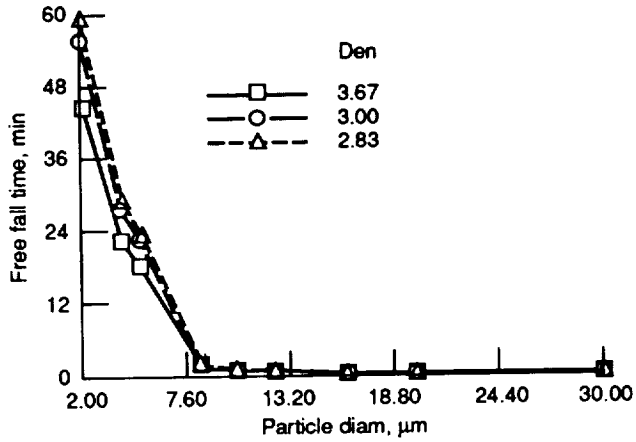

Figure 6.—Falling time versus particle size. Distance = 0.71 meters.

ORIGINAL PAGE
BLACK AND WHITE PHOTOGRAPH

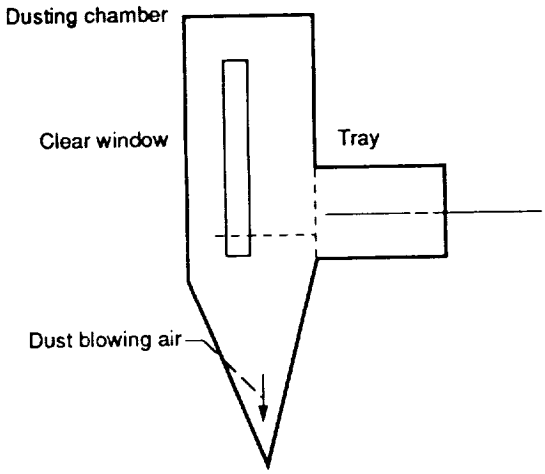

Figure 7.—Dust box.

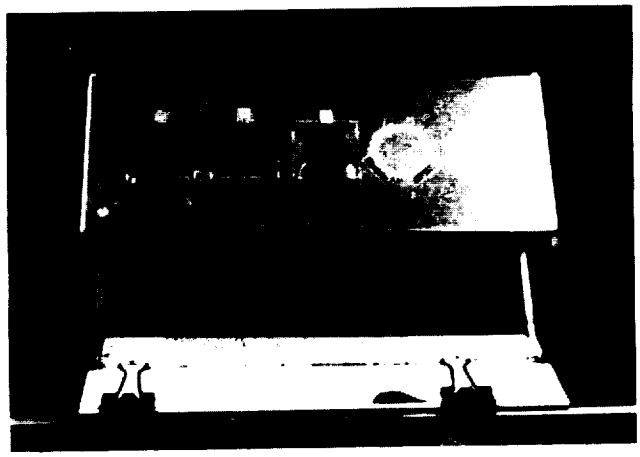

Figure 8.—Samples holder design.

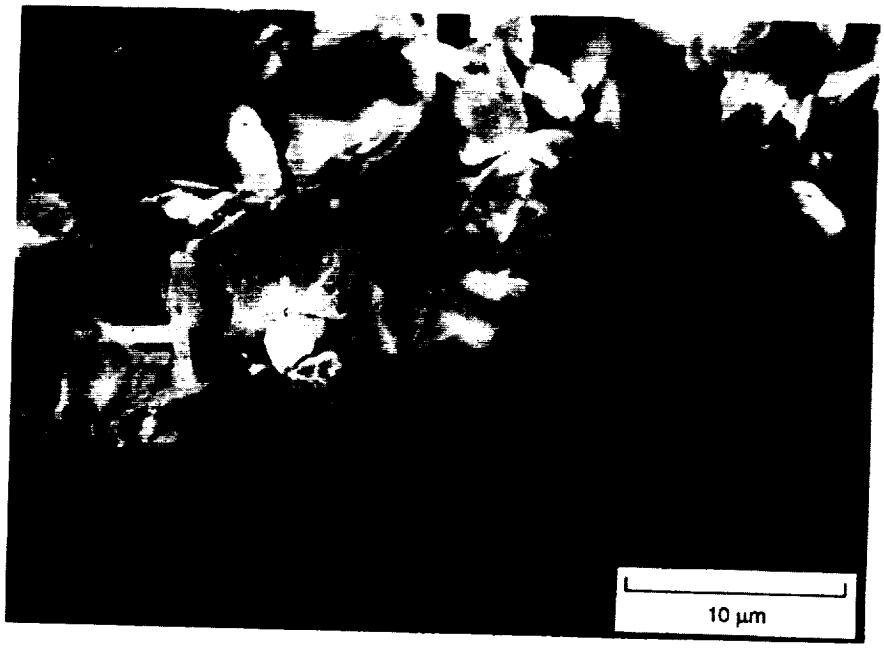

(a) Aluminum Oxide polishing grit.

(b) Basalt.

Figure 9. Scanning Electron Microscopy (SEM) Showing Particle Shape

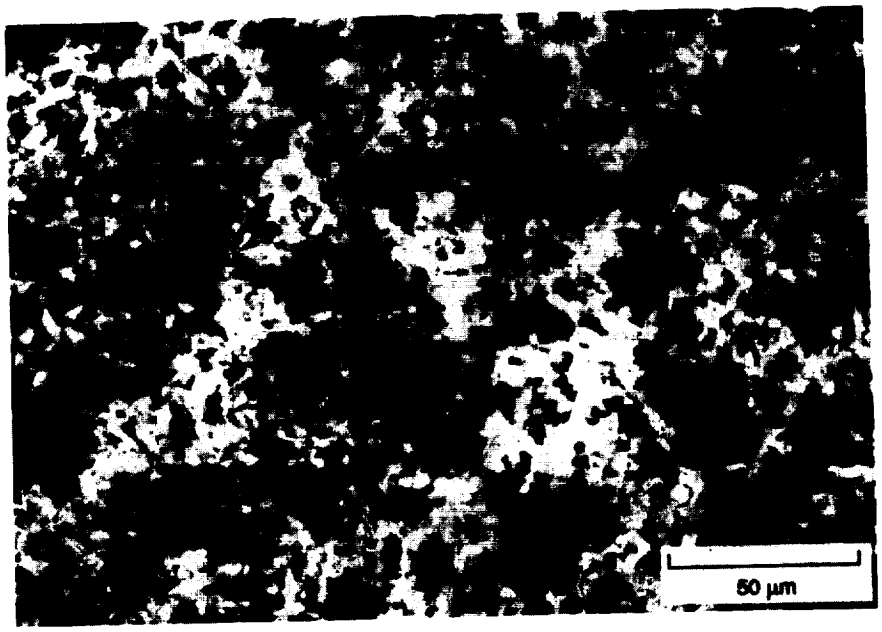

(a) Aluminum Oxide polishing grit.

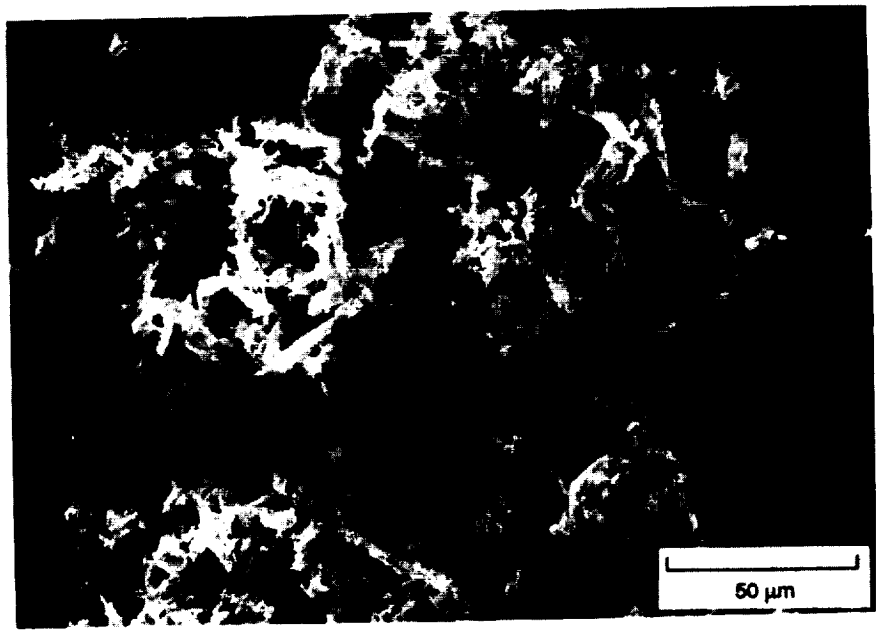

(b) Basalt.

Figure 10. Scanning Electron Microscopy (SEM) of Dusted Samples

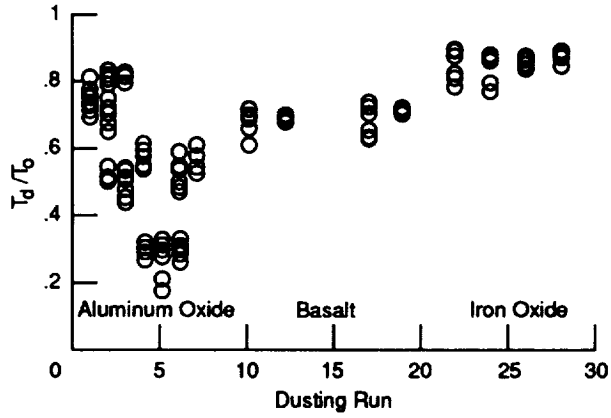

Figure 11. Uniformity of Dust Deposition

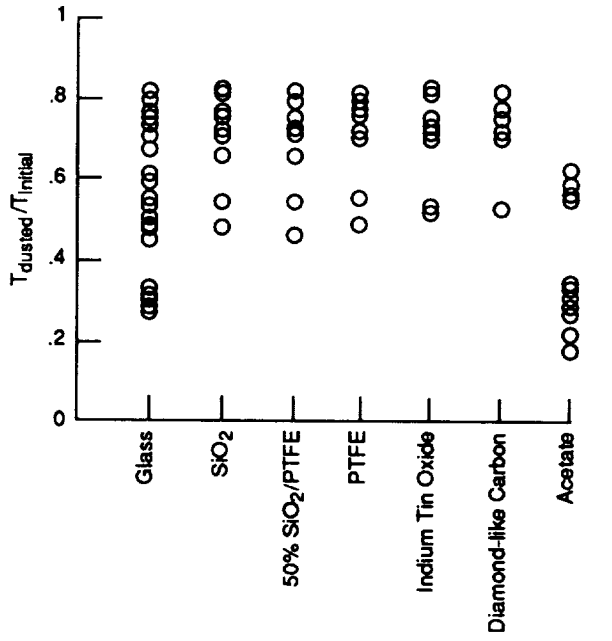

Figure 12. Uniformity of Dust Deposition by Material Using Aluminum Oxide Dust